Archive of Applied Mechanics (2021) 91:4475–4483
https://doi.org/10.1007/s00419-021-02016-x

ORIGINAL

Magdalena Łępicka · Grzegorz Górski · Małgorzata Grądzka-Dahlke · Grzegorz Litak · Bartłomiej Ambrożkiewicz

Analysis of tribological behaviour of titanium nitride-coated stainless steel with the use of wavelet-based methods

Received: 21 August 2020 / Accepted: 2 July 2021 / Published online: 19 July 2021
© The Author(s) 2021

Abstract Tribological behaviour is characterized by the strong nonlinear effects in its response, which are hardly identified with standard signal processing methods. One of the challenges in the analysis of wear phenomena is identification of its propagation and potential quantification. In our study, we propose application of wavelet-based methods, i.e. continuous wavelet transform and scale index for analysis of the dynamical response in the tribological pair. The analysed parameter will be the coefficient of friction, which is slightly changing with wear of the tribological pair. The performed analysis shows the variable response of the system in each considered state. Moreover, results obtained with wavelets are useful for its determination. The proposed methods can be particularly useful in the transportation applications, where the quantification of the friction force between the sliding counterparts is a crucial parameter, responsible for the power losses. Early and efficient identification of wear allows to predict damage and avoid undesirable downtime or time-consuming exchange of a worn out part.

Keywords Tribology · Coefficient of friction · Titanium nitride-coated stainless steel · Wavelet analysis · Scale index

1 Introduction

In the recent decades, a growing interest into improving operational properties of engineering materials with the use of hard anti-wear coatings was seen. One of the films which attracted the most attention is titanium nitride, which has been introduced into the market more than a half century ago [1]. Since then, titanium nitride was used in machine industry in various industrial applications.

However, though thin films can significantly improve reliability of machinery, it was proven that once the protective film is damaged, a substantial intensification in wear processes can be observed [2]. Therefore, it is crucial to be able to detect the changes that occur in the system when the film fails. Nevertheless, regardless of numerous attempts to solving the issue of detection of the film failure and developing sophisticated methods for film damage identification [3, 4], the above problem is still actual.

According to [5], the friction-induced transition between the wear modes of a coupled tribopair is reflected in changes in its oscillations. It was shown that the friction-induced vibrations show different characteristics for different wear mechanisms [5]. Nevertheless, identification of wear-related vibrations of a mechanical system

M. Łępicka · G. Górski (✉) · M. Grądzka-Dahlke
Institute of Mechanical Engineering, Faculty of Mechanical Engineering, Białystok University of Technology, ul. Wiejska 45C, 15-351 Białystok, Poland
e-mail: g.gorski@pb.edu.pl

G. Litak · B. Ambrożkiewicz (✉)
Faculty of Mechanical Engineering, Lublin University of Technology, Nadbystrzycka 36, 20-618 Lublin, Poland
e-mail: b.ambrozkiewicz@pollub.pl

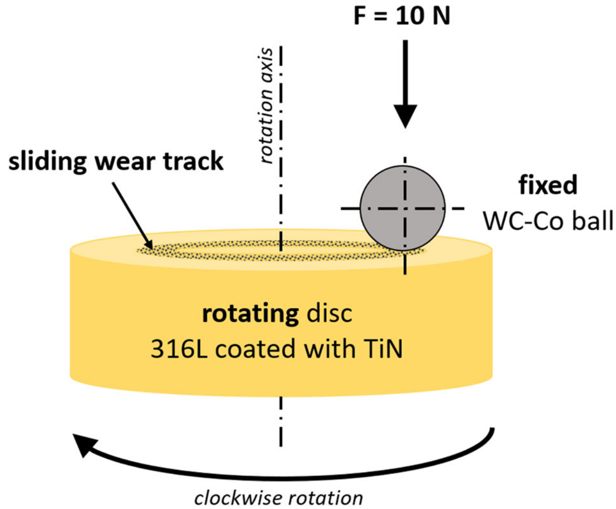

Fig. 1 Schematic representation of the ball-on-disc wear test system

is a complex challenge. In the work by Spurr et al. [6], it was mentioned that oscillations of a tribosystem can fall into two categories. First, the vibrations can be induced due to the geometrical characteristics of a system. When wear between mating surfaces occurs, the kinematic coupling between the variation in normal and friction forces arises. Second, the stick–slip behaviour of a system will produce instabilities of the friction coefficient. According to Sinou et al. [7], transitions between static and dynamic friction will cause the saw-tooth like vibrations of a frictional system.

Therefore, vibrations that are generated in the system, because of friction, provide information that reflect not only the current state, but also the features of a tribological pair [5]. One of the methods for extracting the transient features of a tribosystem is the wavelet analysis. The application of wavelet method for studying the dynamical characteristics of a system has previously been proposed in tribology, e.g. for the purpose of diagnosis of failure of a rolling bearing [8]. In this study, the dynamic characteristics of friction coefficient obtained for TiN-coated 316LVM steel were analysed with the use of the wavelet method.

As the tribological wear is changing and propagating in time, one of the most efficient methods for its analysis is wavelet-based methods. They have already been used in fault diagnostics of plenty of mechanical systems such as gears [9, 10], bearings [11, 12] or shafts [13, 14]. In our case, we consider the tribological problem, which occurs in model ball-on-disc frictional tests. In this type of a frictional study, a simple tribological contact is used. Due to simplicity of the method, as well as repeatability of the obtained data, those types of tests are being done to assess the anti-wear performance of thin films.

Till now, several papers on identification of wear phenomena with wavelet transform were published for different tribosystems. For example, some attention has been paid to wavelet-assisted detection of failure of ball bearings. Attoui et al. proposed the combination of wavelet-discriminant method for the identification of damaged element in ball bearings [15], Puche-Panadero et al. proposed to apply the numerical method combining the wavelet transform, the Wigner Viller distribution and Hilbert transform in fault diagnosis of induction machines [16]. One of the most important issues in the tribological studies is not only the identification of failure caused by wear, but also the relatively early prevention of severe wear of a tribosystem. In our study, we propose the method based on combination of the continuous wavelet analysis (CWT) and scale index, as the measure of the periodicity of the signal. The dynamical response of found tribological state differs from each other, what can be easily detected with CWT, but the scale index provides the crucial and useful information on the severity of wear by quantitative determination of nonlinearities in the system, which correspond to a specific state in the tribological pair.

In this paper, we describe results from experimental data obtained from a wear test, as well as the tribological behaviour of the tribopair. First, in the next section, we describe the experimental setup and data acquisition in the experiment. Then, in Sects. 3 and 4, respectively, we describe the wavelet-based methods (CWT and Scale Index), along with the results from the analysis of the experimental signal for measured coefficient of friction (COF). In the end, in Sect. 5, we, Fig. 1, summarize our conclusions and suggestions for application of proposed methods and future research.

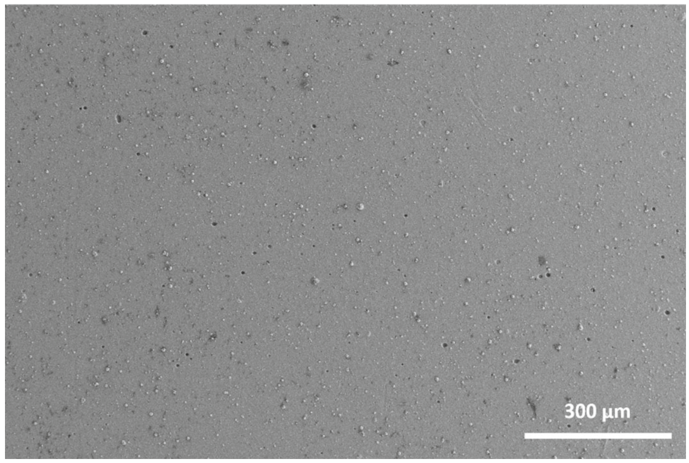

Fig. 2 SEM micrograph of the sample surface obtained prior to starting the wear test

2 Experimental setup

For the dry wear test, 316L stainless steel was selected as the substrate material. Mirror-polished, 6-mm-thick discs were fabricated from a Ø25 mm bar. After that, samples were thoroughly cleaned and coated with a commercial titanium nitride film, which has been prepared with the use of physical vapour deposition (PVD) techniques. The film thickness was approximately 2 µm. The surface roughness parameters of the samples were measured after the coating deposition with the use of a contact profilometer. The Ra was equal to 0.044 µm, while Rt = 0.037 µm. The SEM image of the surface state before starting the tribological test is given in Fig. 2. As can be seen in Fig. 2, some surface irregularities are seen on the sample surface. Their presence is caused by the nature of the PVD deposition process.

The wear test was conducted on a CSM Instruments (Switzerland) microtribometer, in a ball-on-disc configuration (Fig. 1). The frictional test parameters were based on our previous experiences collected during the wear tests conducted on TiN-coated steels. Therefore, the test was done in dry conditions, in an ambient temperature and humidity. As the counter material, a fixed Ø6 mm WC–Co ball (Ceramit, Poland) was used, while the TiN-coated Ø25 $\times$ 6 mm discs were working in the rotating mode. The sliding velocity was equal to 10 cm/s. Before the tribological test, all considered samples were thoroughly cleaned in a sonicator. The following cleaning agents were used: acetone, isopropanol and deionized water.

During the frictional test, a normal load of 10 N was applied on a WC–Co ball, which was fixed in the tribometer arm (Fig. 1). The rotational movement in the clockwise direction was done by a TiN-coated disc. The diameter of the sliding track is equal to 6 mm. The resulting coefficient of friction of the tribological pair was recorded with the frequency of 20 Hz.

3 Wavelet analysis

The approach to the evaluation of the dynamic character of the tribological behaviour obtained in the experiment is the wavelet analysis. The method found its application in many areas of science, such as engineering [17, 18], medicine [19, 20], chemistry [21, 22] or materials science [23, 24] and is especially used in the detection of rapidly changing transient states or intermittencies in the analysed systems. The wavelet transform shows some advantages over the fast Fourier transform (FFT) [25] and its modification based on window analysis, the so-called short-time Fourier transform (STFT). The wavelet transform provides simultaneous analysis in time and frequency domain. FFT instead reveals the characteristic frequencies present in the spectra, but it does not provide the information of how are they changing in time. The STFT approach is very similar in comparison with WT, but it is limited with the fixed-size window [26] taken for signal processing. In the STFT, both the frequency and the time resolution are fixed by the applied window-size in the analysis, so that the periodicities in the time series can be poorly detected, what matters in analysis of transient and rapidly changing states.

The wavelet analysis is an adaptive method to the dynamic situation in the system, depending on the applied type of wavelet, characterizing with the time and frequency resolutions. The applied window narrows when focusing on small-scale or high-frequency features of the signal and broadens on large-scale or low-frequency features, showing it in a compact form on the scalogram. Moreover, wavelets offer revealing aspects of data, such as identification of trends, breakdown points and discontinuities in higher derivatives and self-similarity. The formal definition of a wavelet is that it is a small wave with a compact support and it can be treated as the wavelet, when the function $\psi(t)$ should have zero mean and finite energy. The continuous wavelet transform (CWT) of the experimental time series$\mu(t)$ with respect to a mother wavelet is given by a convolution of the time series with a scaled and translated version of applied wavelet. It can be described as follows:

$$W_{s,n}(\mu) = \sum_{i-1}^{N} \frac{1}{s} \psi\left(\frac{i-n}{s}\right) \frac{(\mu(t_i) - \langle\mu\rangle)}{\sigma_\mu}, \quad (1)$$

where $< \mu >$ and σ_μ are the averages and standard deviation of COF, the variables *s* and *n* denote the scale and the time indices, respectively. The scale parameter is responsible for the dilation ($s > 1$) and the contraction ($s < 1$) of applied mother wavelet. The role of the time index *n* is finding the position of the wavelet in time.

The wavelet power spectrum [27, 28] is defined as the square modulus of the continuous wavelet transform and is as follows:

$$P_w = \left|W_{s,n}\right|^2 \quad (2)$$

The WPS value is dependent on scales, frequencies and time and can be determined as the variance in specific scale or frequency. This is clearly visible on corresponding scalograms. The measure is useful in the analysis of non-stationary data, as obtained in the experiment. From many different types of wavelets, we applied to the calculations, the complex Morlet wavelet [29–31], defined with Gaussian shape and the central frequency $\omega_0 = 6$. This value provides a good balance between time and frequency localizations. For $\omega_0 = 6$, the Fourier period is approximately equal to the scale *s*.

One of the promising wavelet-based tools allowing to identify the periodicity of the signal is the scale index (SI) [32, 33]. The inner scalogram of analysed time series μ is described as follows:

$$S(s) = (\int_{c(s)}^{d(s)} |W\mu(u,s)|^2 du/(d(s) - c(s))^{\frac{1}{2}} \quad (3)$$

where $W\mu(u,s)$ is the continuous wavelet transform (CWT) of time series at the specified time *u* and scale *s*. Next, the scale index in the scale interval $[s_0,s_1]$, is calculated as the quotient:

$$i_{scale} = \frac{S(s_{min})}{S(s_{max})}, \quad (4)$$

where s_{max} is the maximum estimated in the specified scale interval$[s_0,s_1]$, and s_{min} is the minimum in the interval $[s_{max}s_1]$. The value of scale index can be from the range [0,1], quantifying the level of non-periodicity of the signal. The result of the SI to it denotes high level of non-periodicity, instead it is equal to 0 or close to it, the signal has periodic character.

4 Results of data analysis

With help of the wavelet-based methods, we obtained qualitative and quantitative changes of the COF response illustrated in Fig. 3. The surface profile of the wear scar collected at the end of the frictional test is shown in Fig. 4. Taking into account the thickness of the TiN film (2 μm), it can be clearly seen that the protective coating was worn off the sample surface as a result of frictional action between the counter sample and the disc.

However, based on the nature of the frictional time series, we distinguished three specific dynamic states (developed in fairly long intervals) that can be observed during a tribological test, i.e. A) running-in, where the initial surface irregularities are being worn out, B) stabilized friction, when wear of the material progresses steadily in time and C) instable wear, when we observe intermittent character of the COF response. The dynamics of the time series were divided accordingly to our previous paper [34]. All three observed states are very similar in quantitative way, that is why it is justified to apply wavelet and scale index analysis in order to define them by the periodicity level of the dynamical response.

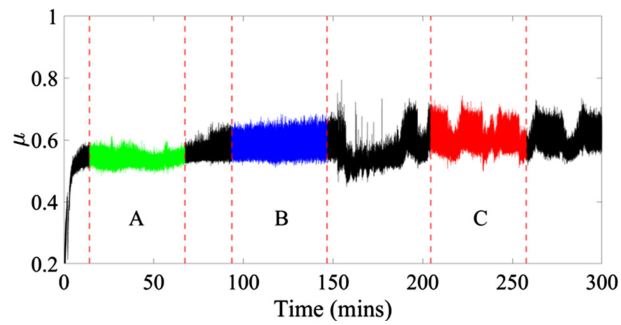

Fig. 3 Time series obtained from the COF measurements in time domain. The three specific tribological states behaviour are marked: A—the running-in (green), B—stabilized friction (blue) and C—instable wear (red)

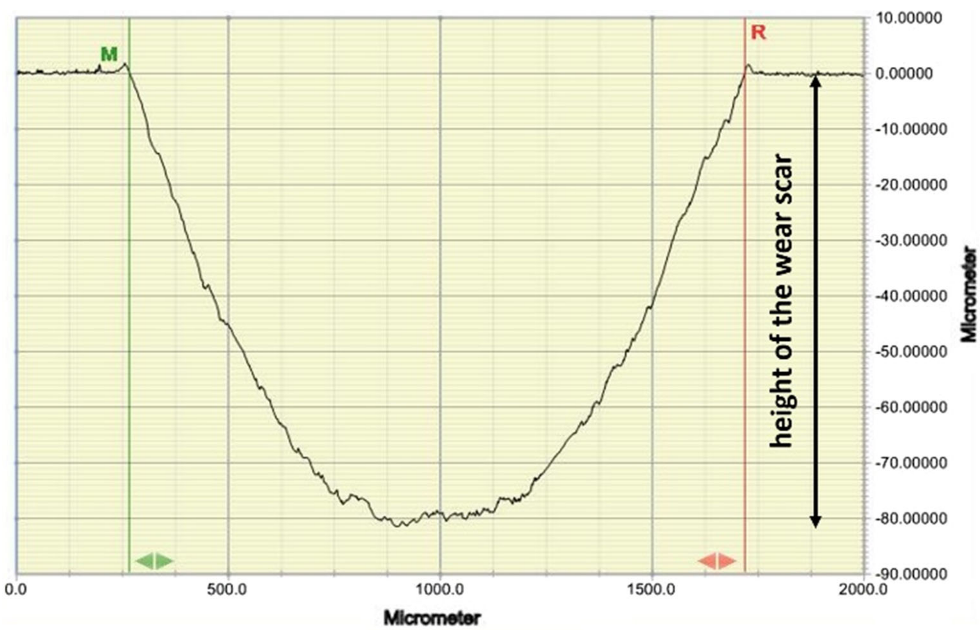

Fig. 4 Cross-sectional profile of the wear scar obtained for TiN-coated 316L steel. The profile was collected with the use of a contact surface profilometer

On the scalograms (Fig. 5), the changes of the COF signals in every state can be clearly observed in time–frequency domain. Clearly, the dominating characteristic frequency in all cases is close to 8 Hz, but it is caused by sampling frequency. The rest of character of magnitudes in the scalograms differ from case to case. Note that, we observe distributed local intervals of white colour, in the contrast with blue backgrounds. Here, the blue colour represents the smaller, while the white colour—the higher wavelet power levels. The colour scale between them denotes the intermediate power level. The red colour indicates the highest level of wavelet power and it is present as isolated points only in the region of 8 Hz. In case of the running-in state, temporary and intermittent amplification gains are observed at a characteristic frequency, but also at low frequencies, what can be ascribed as the presence of noise in the spectra. During stabilized friction, the intermittences disappear. In the scalogram of the last considered state, the share of intermittent behaviour is significant. In the time domain, we can observe not only the main frequency, but temporary power spectra amplifications in wider range of frequencies. The same, non-periodic character can be observed in the raw signal. However, in order to unambiguously distinguish the states from each other in quantitative way, application of SIA method is needed. The time series (Fig. 3) and wavelet scalograms (Figs. 5a and c) show the nonlinear correlations, presumably induced by friction disturbances. The wavelet analysis indicates some of instabilities. Firstly, in Fig. 5a, we observe the periodic instabilities of low frequency, while in Fig. 5b of about 0.05 Hz. Secondly, in Fig. 5a, the instabilities of broader frequency ranges are localized in the fairly short time intervals, represented by the white colour.

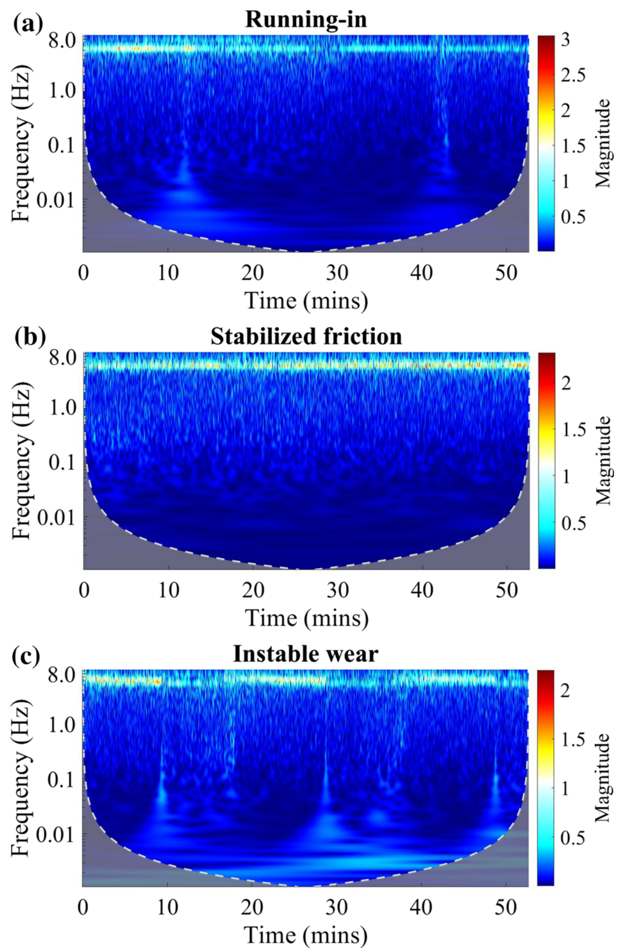

Fig. 5 Wavelet results of the COF measurements for cases presented in Fig. 2, **a** running-in, **b** stabilized friction, **c** instable wear. The scale on the right-hand side denotes the increase in the wavelet power. The regions below the U-shape curve denote the cone of influence. Outside this cone, the edge effects are important and such region is removed from the discussion. The cases **a**–**c** are consistent with cases denoted in Fig. 2 by A, B and C, respectively.

The effects of above instabilities can also be visible in the corresponding return maps [35], plotted in Fig. 6. These plots are close to a circular shape, informing about fairly strong stochastic components in the studied time series. Consequently, the larger circular area in points distribution indicates the higher stochastic influence (as visible in Fig. 6b). Additional distortions caused by the frictional instabilities influence the distributions (Fig. 6a and c) of the signal, in the presence of nonlinear correlations.

In the following step, it is reasonable to perform scale index analysis (SIA). The limit of small scale involves the sampling noise oscillations. Therefore, to estimate the inner scalograms, we limit to lower frequencies from the interval [0.001 Hz, 0.01 Hz]. Consequently, periodic tendencies of the signals can be clearly identified in Fig. 7. The corresponding scale index i_{scale} was estimated as 0.181, 0.198, 0.275, for cases A, B, and C, respectively.

The highest level of the non-periodicity is obtained for the unstable friction (C). In case of running-in case (A), we observe smaller maximum with respect to C. For the stable wear state (B), the value of scale index has a decreasing trend, proving the presence of lower non-periodicity level in the signal. It is related to the vanishing fluctuations of COF within considered frequency ranges. It is worth to notice that observations based on obtained scalograms and scale index values are convergent. Based on mentioned tools, we are able to roughly identify the current tribological state of a system.

Note that, the investigated time series are very noisy (Fig. 3). In terms of wavelets, this effect is visible as the background. Additional disturbances in the time series (In Fig. 2, 3a and c) show the nonlinear correlations, which can be visible in the corresponding return maps [33]. Note that, largest circular area in points distribution

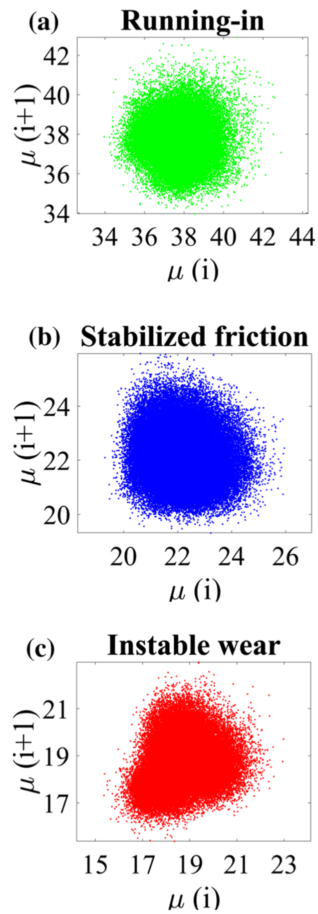

Fig. 6 Return maps based on the measured friction coefficient μ. Note that, largest circular area in points distribution indicates a high stochastic influence **b** while distortions in the distributions **a** and **c** signal the presence of nonlinear correlations. Colours are consistent with cases denoted in Fig. 2.

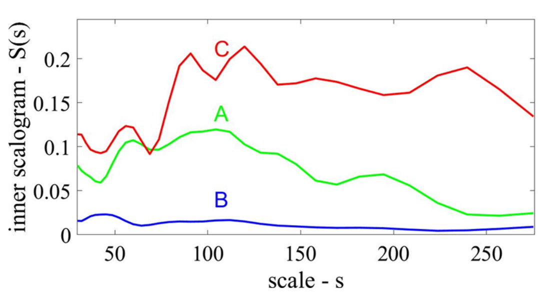

Fig. 7 Normalized inner scalograms for the tribological behaviours. The green line denotes the running-in state, blue the stabilized friction and red the instable wear. Colours are consistent with cases denoted in Fig. 2. The scale index i_{scale} was estimated as 0.181, 0.198, 0.275, for cases A, B and C, respectively. The scale interval corresponds to the frequency limits [0.001 Hz, 0.01 Hz].

indicates a highly stochastic influence (Fig. 4b), while distortions in the signal distributions (Fig. 6a and c) are a sign of the presence of nonlinear correlations. These correlations influence the time response of the investigated system, which can be identified by the corresponding scale indexes based in inner scalograms (Fig. 7). Note that, the case B (Fig. 3) is characterized by the oscillations without visible scale preferences, besides the fairly small-scale limit.

5 Conclusions

By application of continuous wavelet transform (CWT) and scale index analysis (SIA), we have demonstrated that wavelet-based methods allow to distinguish different tribological states that occur during tribological test of a titanium nitride-coated stainless steel. In obtained scalograms, by changing value of wavelet power spectra (WPS), it was possible to detect the transient states found in the raw signals from measurements of the coefficient of friction (COF). The TiN coating was wearing in time resulting in the non-monotonic changes of roughness. After initial decrease in roughness in a stabilized friction phase, we could obtain higher roughness in an instable wear phase. Due to this effect, friction coefficient is modulated by low-frequency components. This is consistent with the observations in CWT analysis. The proposed methods are very useful not only considering the time-domain analysis, but also analysis at very low frequencies, as we had in the experiment. The results of scale index analysis proved that with the onset of new friction and wear processes, e.g. three-body abrasion, oxidation, removal of oxygen-rich layers and adhesion, as well as their mutual interactions, we obtain the response with higher influences of the nonlinear effects.

Referring to the previous applied methods, i.e. recurrence quantification analysis (RQA) and principal component analysis (PCA) [34], the wavelet-based methods can be their alternative in the manner of the tribological states detection. However, the scale index analysis provides the quantitative information about the level of wear corresponding the COF value. More advanced investigations on the wear of the coated systems, comprising with statistical methods, would allow to create the classification based on results obtained from the scale index analysis. Certainly, proposed direction of the future research could become the part of Industry 4.0 concept and applied exemplary as the neural network in an actual application.

Acknowledgements The work was supported by the National Science Centre (Republic of Poland) within the PRELUDIUM 13 grant proposal, project no. UMO-2017/25/N/ST8/02270. The work was also supported by WZ/WM-IIM/2/2020.

Declarations

Conflict of interest The authors declare that they have no conflict of interest.

Open Access This article is licensed under a Creative Commons Attribution 4.0 International License, which permits use, sharing, adaptation, distribution and reproduction in any medium or format, as long as you give appropriate credit to the original author(s) and the source, provide a link to the Creative Commons licence, and indicate if changes were made. The images or other third party material in this article are included in the article's Creative Commons licence, unless indicated otherwise in a credit line to the material. If material is not included in the article's Creative Commons licence and your intended use is not permitted by statutory regulation or exceeds the permitted use, you will need to obtain permission directly from the copyright holder. To view a copy of this licence, visit http://creativecommons.org/licenses/by/4.0/.

References

1. Van Hove, R.P., Sierevelt, I.N., van Royen, B.J., Nolte, P.A.: Titanium-nitride coating of orthopaedic implants: a review of the literature. BioMed Res Int (2015). https://doi.org/10.1155/2015/485975
2. Vera, E.E., Vite, M., Lewis, R., Gallardo, E.A., Laguna-Camacho, J.R.: A study of the wear performance of TiN, CrN, and WC/C coatings on different steel substrates. Wear **271**, 2116–2124 (2011)
3. Zhu, W., Zhang, C.X., Yang, L., Zhou, Y.C., Liu, Z.Y.: Real-time detection of damage evolution and fracture of EB-PVD thermal barrier coatings under thermal shock: An acoustic emission combined with digital image correlation method. Surface Coatings Technol **399**, 126151 (2020)
4. Liu, X.Y., Wei, Y.G., Liang, L.H., Liu, X.H., Wang, Y.B., Long, H.: Damage evolution and fracture of ceramic coating systems in circle plate bending tests: Experimental observation and modelling. Ceram. Int. **46**, 8334–8343 (2020)
5. Li, G., Lin, Y., Wang, H., Wei, H., Wang, G.: Harmonic wavelet packet analysis of friction-induced vibration. Tribol. Trans. **54**, 895–901 (2011)
6. Spurr, R.T.: A theory of brake squeal. Proc. Instit. Mech. Eng. Automobile Division **1**, 33–40 (1961)
7. Sinou, J.-J., Cayer-Barrioz, J., Berro, H.: Friction-induced vibration of a lubricated mechanical system. Tribol. Int. **61**, 156–168 (2013)
8. Zhao, L.-Y., Wang, L., Yan, R.-Q.: Rolling bearing fault diagnosis based on wavelet packet decomposition and multi-scale permutation entropy. Entropy **17**, 6447–6461 (2015)
9. Chen, R., Li, Z., Pan, J., Chen, G., Zi, Y., Yuan, J., Chen, B., He, Z.: Wavelet transform based on inner product in fault diagnosis of rotating machinery: A review. Mech. Syst. Signal Process. **70–71**, 1–35 (2016)
10. Li, C., Sanchez, R.V., Zurita, G., Cerrada, M., Cabrera, D., Vasquez, R.E.: Gearbox fault diagnosis based on deep random forest fusion of acoustic and vibratory signals. Mech. Syst. Signal Process. **76–77**, 283–293 (2016)

11. Chen, J., Pan, J., Li, Z., Zi, Y., Chen, X.: Generator bearing fault diagnosis for wind turbine via empirical wavelet transform using measured vibration signals. Renewable Energy **89**, 80–92 (2016)
12. Chandra, N.H., Sekhar, A.S.: Fault detection in rotor bearing systems using time frequency techniques. Mech. Syst. Signal Process. **72–73**, 105–133 (2016)
13. Xiang, J., Zhong, Y.: A novel personalized diagnosis methodology using numerical simulation and an intelligent method to detect faults in a shaft. Appl. Sci. **6**, 414 (2016)
14. Gomez, M.J., Castejon, C., Corral, E., Garcia-Prada, J.C.: Analysis of the influence of crack location for diagnosis in rotating shafts based on 3 x energy. Mech. Mach. Theory **103**, 167–173 (2016)
15. Attoui, I., Fergani, N., Boutasseta, N., Oudjani, B., Deliou, A.: A new time-frequency method for identification and classification of ball bearing faults. J. Sound Vib. **397**, 241–265 (2017)
16. Puche-Panadero, R., Martinez Roman, J., Sapena-Bano, A., Burriel-Valencia, J., Riera-Guasp, M.: Fault diagnosis in the slip-frequency plane of induction machines in time-varying conditions. Sensors **20**(3398), 1–25 (2020)
17. Sen, A.K., Litak, G., Finney, C.E.A., Daw, C.S., Wagner, R.M.: Analysis of heat release dynamics in an internal combustion engine using multifractals and wavelets. Appl. Energy **87**, 1736–1743 (2010)
18. Lonkwic, P., Łygas, K., Wolszczak, P., Molski, S., Litak, G.: Braking deceleration variability of progressive safety gears using statistical and wavelet analysis. Measurement **110**, 90–97 (2017)
19. Martis, R.J., Acharya, U.R., Min, L.C.: ECG beat classification using PCA, LDA, ICA and discrete wavelet transform. Biomed. Signal Process. Control **8**, 437–448 (2013)
20. Quellec, G., Lamard, M., Cazaguel, G., Cochener, B., Roux, C.: Wavelet optimization for content-based image retrieval in medical databases. Med. Image Anal. **14**, 227–241 (2010)
21. Wang, D., Li, Q., Han, C., Lu, Q., Xing, Z., Yang, X.: Atomic and electronic modulation of self-supported nickel-vanadium layered double hydroxide to accelerate water splitting kinetics. Nat. Commun. **10**, 3899 (2019)
22. Ortiz-Echeverri, C.J., Salazar-Colores, S., Rodriguez-Resendiz, J., Gomez-Loenzo, R.A.: A new approach for motor imagery classification based on sorted blind source sepearation, continuous wavelet transform and convolutional neural network. Sensors **19**, 4541 (2019)
23. Rabi, J., Balusamy, T., Raj, J.R.: Analysis of vibration signal responses on pre-induced tunel defects in friction stir welding using wavelet transform and empirical mode decomposition. Defence Technol **15**, 885–896 (2019)
24. Srivastava, M., Anderson, C.L., Freed, J.H.: A new wavelet denoising method for selecting decomposition levels and noise thresholds. IEEE Access **4**, 3862–3877 (2016)
25. Sifuzzaman, M., Islam, M.R., Ali, M.Z.: Application of wavelet transform and its advantages compared to Fourier transform. J. Phys. Sci. **13**, 121–134 (2009)
26. Kiymik, M.K., Guler, I., Dizibuyuk, A., Akin, M.: Comparison of STFT and wavelet transform methods in determining epileptic seizure activity in EEG signals for real-time application. Comput. Biol. Med. **35**, 603–616 (2004)
27. Kirby, J.F., Swain, C.J.: Power spectral estimates using two-dimensional Morlet-fan wavelets with emphasis on the long wavelengths: jackknife errors, resolution and orthogonality properties. Geophys. J. Int. **194**, 78–99 (2013)
28. Koszałka, G., Hunicz, J., Rysak, A., Litak, G.: Nonlinear vibration of semitrailer suspension: wavelet and multiscale entropy-based approaches. Arch. Appl. Mech. **86**, 761–768 (2016)
29. Cohen, M.X.: A better way to define and describe Morlet wavelets for time-frequency analysis. Neuroimage **199**, 81–86 (2019)
30. Sabir, Z., Wahab, H.A., Umar, M., Sakar, M.G., Raja, M.A.Z.: Novel design of Morlet wavelet neural network for solving second order Lane-Emden equation. Math. Comput. Simul. **172**, 1–14 (2020)
31. Sen, A.K., Longwic, R., Litak, G., Górski, K.: Analysis of cycle-to-cycle pressure oscillations in a diesel engine. Mech. Syst. Signal Process. **22**, 362–373 (2008)
32. Bolos, V.J., Benitez, R., Ferrer, R.: A new wavelet tool to quantify non-periodicity of non-stationary economic time series. Mathematics **8**, 844 (2020)
33. Benitez, R., Bolos, V.J., Ramirez, M.E.: A wavelet-based tool for studying non-periodicity. Comput. Math. Appl. **60**, 634–641 (2010)
34. Łępicka, M., Górski, G., Grądzka-Dahlke, M., Mosdorf, R.: Study of tribological behaviour of surface modified stainless-steel using recurrence quantification analysis and principal component analysis. Tribol. Int. **151**, 106402 (2020)
35. Sprott J.C.: Chaos and time-series analysis. Oxford University Press (2003)

Publisher's Note Springer Nature remains neutral with regard to jurisdictional claims in published maps and institutional affiliations.